

Study of D^0 decays into final states with a π^0 or η

K. Kinoshita,^a F. M. Pipkin,^a M. Procaro,^a Richard Wilson,^a J. Wolinski,^a D. Xiao,^a
 Y. Zhu,^a R. Ammar,^b P. Baringer,^b D. Coppage,^b R. Davis,^b P. Haas,^b M. Kelly,^b
 N. Kwak,^b Ha Lam,^b S. Ro,^b Y. Kubota,^c J. K. Nelson,^c D. Perticone,^c R. Poling,^c
 S. Schrenk,^c G. Crawford,^d R. Fulton,^d T. Jensen,^d D. R. Johnson,^d H. Kagan,^d R. Kass,^d
 R. Malchow,^d F. Morrow,^d J. Whitmore,^d P. Wilson,^d D. Bortoletto,^e D. Brown,^e J. Dominick,^e
 R. L. McIlwain,^e D. H. Miller,^e M. Modesitt,^e C. R. Ng,^e S. F. Schaffner,^e E. I. Shibata,^e I. P. J. Shipsey,^e
 M. Battle,^f H. Kroha,^f K. Sparks,^f E. H. Thorndike,^f C.-H. Wang,^f M. S. Alam,^g I. J. Kim,^g
 W. C. Li,^g V. Romero,^g C. R. Sun,^g P.-N. Wang,^g M. M. Zoeller,^g M. Goldberg,^h T. Haupt,^h
 N. Horwitz,^h V. Jain,^h M. D. Mestayer,^h G. C. Moneti,^h Y. Rozen,^h P. Rubin,^h T. Skwarnicki,^h
 S. Stone,^h M. Thusalidas,^h W.-M. Yao,^h G. Zhu,^h A. V. Barnes,ⁱ J. Bartelt,ⁱ S. E. Csorna,ⁱ
 T. Letson,ⁱ J. Alexander,^j M. Artuso,^j C. Bebek,^j K. Berkelman,^j D. Besson,^j T. Browder,^j
 D. G. Cassel,^j E. Cheu,^j D. M. Coffman,^j P. S. Drell,^j R. Ehrlich,^j R. S. Galik,^j M. Garcia-Sciveres,^j
 B. Geiser,^j B. Gittelman,^j S. W. Gray,^j A. M. Halling,^j D. L. Hartill,^j B. K. Heltsløy,^j K. Honscheid,^j
 J. Kandaswamy,^j N. Katayama,^j D. L. Kreinick,^j J. D. Lewis,^j G. S. Ludwig,^j J. Masui,^j J. Mevissen,^j
 N. B. Mistry,^j S. Nandi,^j E. Nordberg,^j C. O'Grady,^j D. Peterson,^j M. Pisharody,^j D. Riley,^j
 M. Sapper,^j M. Selen,^j A. Silverman,^j H. Worden,^j M. Worris,^j A. J. Sadoff,^k P. Avery,^l
 L. Garren,^l and J. Yelton^l

(The CLEO Collaboration)

^aHarvard University, Cambridge, Massachusetts 02138^bUniversity of Kansas, Lawrence, Kansas 66045^cUniversity of Minnesota, Minneapolis, Minnesota 55455^dOhio State University, Columbus, Ohio 43210^ePurdue University, West Lafayette, Indiana 47907^fUniversity of Rochester, Rochester, New York 14627^gState University of New York at Albany, Albany, New York 12222^hSyracuse University, Syracuse, New York 13244ⁱVanderbilt University, Nashville, Tennessee 37235^jCornell University, Ithaca, New York 14853^kIthaca College, Ithaca, New York 14850^lUniversity of Florida, Gainesville, Florida 32611

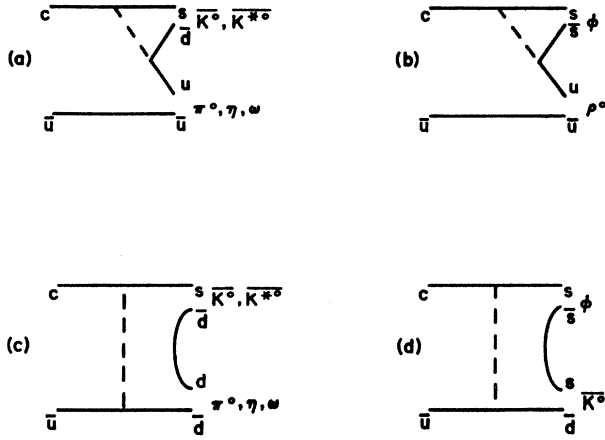
(Received 18 December 1990)

We have made measurements of decay modes of neutral D mesons into exclusive final states containing photons using data collected with the CLEO detector at the Cornell Electron Storage Ring. We report observation of $D^0 \rightarrow K^- \pi^+ \pi^- \pi^+ \pi^0$ (charge conjugates are implicit), and present new measurements of the branching ratios for $D^0 \rightarrow K^- \pi^+ \pi^0$, $D^0 \rightarrow \bar{K}^0 \pi^+ \pi^0 \pi^-$, $D^0 \rightarrow \bar{K}^0 \pi^0$, $\bar{K}^{*0} \eta$, and $D^0 \rightarrow \bar{K}^0 \omega$. Where possible, results are compared with theoretical predictions for two-body D^0 decays.

INTRODUCTION

Among the earliest puzzles in charmed-meson decay was the observation of a much longer lifetime ($\times 2.5$) for the D^+ relative to the D^0 mesons¹ together with widely differing semileptonic branching ratios. In fact, the ratio of lifetimes is the same as the ratio of semileptonic branching ratios (such that the semileptonic rates are equal), indicating that the answer to the lifetime discrepancy must be sought in studies and theoretical consideration of the hadronic decays of the D^0 and D^+ mesons.

In the model of Bauer, Stech, and Wirbel² (BSW), for example, negative interference between the "external" and "internal" spectator decays for the D^+ is considered to be the primary reason for the lower hadronic decay rate for D^+ 's relative to D^0 's. The rate for the decay $D^0 \rightarrow K^- \pi^+$, believed to occur through external W emission, can be used to fix the amplitude of the external spectator diagram; the decay $D^0 \rightarrow \bar{K}^0 \pi^0$ correspondingly defines the amplitude of the internal spectator decay. The decay $D^+ \rightarrow \bar{K}^0 \pi^+$, which is accessible through both diagrams, can be used to determine the interference between the two diagrams.

FIG. 1. D^0 decay diagrams.

It is only within the last several years that sufficient statistics have been accumulated to test models such as the BSW model. Evidence for the decays $D^0 \rightarrow K^0 \bar{K}^0$ (Ref. 3) and $D^0 \rightarrow \phi K_S^0$ (Ref. 4) indicated that the simplest picture of D^0 decay, where all diagrams except the spectator are neglected, must be revised to include contributions from exchange diagrams as well as final-state rescattering. The former decay, predicted to be identically zero in exact SU(3), has been observed at a branching ratio of 0.1%, suggesting the presence of final-state interactions. The branching ratio for the decay $\phi \bar{K}^0$ is zero in the BSW model, in conflict with measurement ($\approx 0.85\%$). The decays $D^0 \rightarrow \bar{K}^0 \omega$ and $D^0 \rightarrow \bar{K}^{*0} \eta$ are, in principle, very similar to $D^0 \rightarrow \bar{K}^0 \pi^0$, but with different spin and isospin structures. These modes are also accessible through the exchange diagram and therefore also give information on nonspectator effects. Figure 1 illustrates some of the D^0 decays we are investigating.

DATA SAMPLE AND EVENT SELECTION

The data sample used consists of 102 pb^{-1} of data at energies just below the $\Upsilon(4S)$, 212 pb^{-1} at the $\Upsilon(4S)$, and 114 pb^{-1} at the $\Upsilon(5S)$ collected with the CLEO detector. We will briefly describe the detector in its configuration during the data taking relevant to this analysis: Charged-particle tracking is performed inside a superconducting solenoid of radius 1.0 m which produces a 1.0-T magnetic field. Three nested cylindrical drift chambers measure momenta and specific ionization for charged particles. The innermost part of the tracking system is a three-layer straw tube vertex detector which gives a position accuracy of $90 \mu\text{m}$ in the r - ϕ plane. The middle ten-layer vertex chamber measures the position with an accuracy of $90 \mu\text{m}$ in the r - ϕ plane and specific ionization (dE/dx) to 14%. The main drift chamber⁵ contains 51 layers, 11 of which are at stereo angles of 1.9° – 3.5° to the z axis, providing an r - ϕ position accuracy of $110 \mu\text{m}$ and dE/dx to 6.5%. Measurements of the track coordinates

along the beam position (z) are achieved by using the stereo layers and cathode strip readouts in the middle vertex chamber and the main drift chamber. Taken together, the system achieves a momentum resolution given by

$$(\delta p/p)^2 = (0.23\%p)^2 + (0.7\%)^2,$$

where p is in GeV/ c . Photons are detected in the barrel electromagnetic calorimeters, which cover 47% of the solid angle and have an energy resolution of $\sigma_E/E = 21\%/\sqrt{E}$ (GeV). The angular resolution of the calorimeter is approximately 10 mrad.

Hadronic events are selected using criteria which have been discussed in detail elsewhere.⁶ Most importantly, we require three or more tracks emanating from a point close to the known primary vertex, along with the deposition of more than 250 MeV of energy in the barrel shower calorimeter. We require that each particle have a dE/dx pulse height in the drift chamber which is within ± 2.5 standard deviations of the assumed particle identity (either π , K , or p). Photons are defined as showers with observed energies in excess of 100 MeV which are contained within the fiducial volume of the barrel calorimeter and which are unmatched (within 0.1 rad) to the impact point of charged tracks extrapolated out of the drift chamber into the barrel calorimeter. If a pair of photons has a mass within 2σ ($\sigma \approx 30$ MeV) of 135 MeV, we call it a π^0 candidate. We then perform a kinematic fit on the photon pair, constraining the mass to the π^0 mass. Our π^0 detection efficiency is typically 15% for π^0 's from D^0 's above x values ($x = p/p_{\text{max}}$) of 0.5. This detection efficiency is primarily due to the product of geometric acceptance ($\approx 50\%$), loss due to photons merging at high x values ($\approx 50\%$), and the reconstruction efficiency for each fiducially contained photon ($\approx 80\%$). We note that, for D^0 modes which include the detection of neutrals, the D^0 mass resolution is substantially degraded by the poor photon-energy resolution. Whereas D^0 's detected in all-charged modes typically have a mass resolution of 30 MeV [full width at half maximum (FWHM)], the inclusion of a π^0 can increase this value by a factor of 3–4, making the direct observation of the D^0 a formidable task. We can reduce the background substantially and improve our sensitivity by requiring the D^0 to come from a parent D^{*+} in the decay $D^{*+} \rightarrow D^0 \pi^+$. We therefore plot the difference in mass (hereinafter referred to as " ΔM ") between the D^0 and the D^{*+} . The resolution in ΔM is typically 2 MeV (FWHM) for the modes of interest. In all that follows, we will require D^0 (defined to lie within 2σ of the D^0 mass) candidates to be D^{*+} daughters. We determine ΔM by combining the candidate D^0 with another pion in the same event. The background is taken into account by considering the D^0 sidebands (defined as 2.5 – $4.5\sigma_D$ on either side of the D^0 , where σ_D depends on the mode we are investigating). Also critical in suppressing the background is the imposition of the requirement $x_D > 0.5$. This requirement preferentially selects charmed particles, which have hard fragmentation functions. In Fig. 2, we plot the D^0 candidate mass versus ΔM for four of the D^0 decay modes.

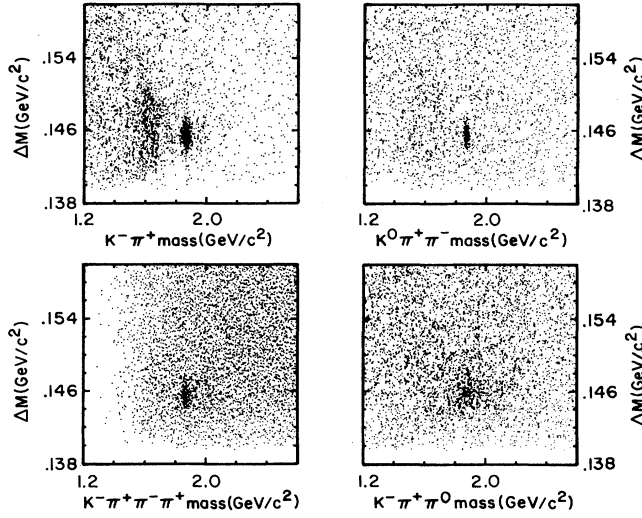


FIG. 2. D^0 candidate mass (horizontal axis) vs ΔM mass (vertical axis) for $D^0 \rightarrow K^- \pi^+ \pi^0$, $D^0 \rightarrow K_S^0 \pi^+ \pi^-$, $D^0 \rightarrow K^- \pi^+ \pi^- \pi^+$, and $D^0 \rightarrow K^- \pi^+ \pi^0$.

We use the decay modes into all-charged final states for purposes of normalization. It is obvious from these plots that there are signals in all channels. It is also evident that the peak for the $D^0 \rightarrow K^- \pi^+ \pi^0$ mode is substantially broader (as is ΔM) than for the all-charged decay modes.

THE DECAYS $D^0 \rightarrow K^- \pi^+ \pi^0$ AND $D^0 \rightarrow \bar{K}^0 \pi^0$

Since we expect the decays $D^0 \rightarrow K^- \pi^+ \pi^0$ and $D^0 \rightarrow \bar{K}^0 \pi^0$ to have high signal-to-noise ratios, we can use these decays to verify that we understand the π^0 detection efficiency by comparing our branching ratios with previously tabulated results.⁷ In Fig. 3, we display ΔM for events fitting $D^0 \rightarrow K_S^0 \pi^0$ and the $K_S^0 \pi^0$ invariant mass for events having ΔM consistent with a D^0 originating from a D^{*+} . In order to determine the number of events for $D^0 \rightarrow K^- \pi^+ \pi^0$ and $D^0 \rightarrow K_S^0 \pi^0$, we fix the means and widths of the D^0 signals according to values obtained from studies of Monte Carlo events, and fit the background according to two estimations of the background beneath the signal. In one case, we use a simple second-order polynomial to approximate the background shape in the ΔM plot; in the second case, we plot the ΔM distribution for events in the D^0 sidebands. The discrepancy between these two algorithms gives us an estimation of the systematic dependence of our final result on the fitting technique used. As another check on systematics, we compare the number of candidate events obtained by fitting the ΔM distribution after the D^0 requirement to the number obtained by fitting the D^0 distribution after the ΔM requirement. We attribute a typical systematic error of 10% arising from whether we fit the ΔM distribution or the D^0 mass distribution; the remainder of the systematic error originates in the parametrization of the background shape, as well as our choice of x cut for the

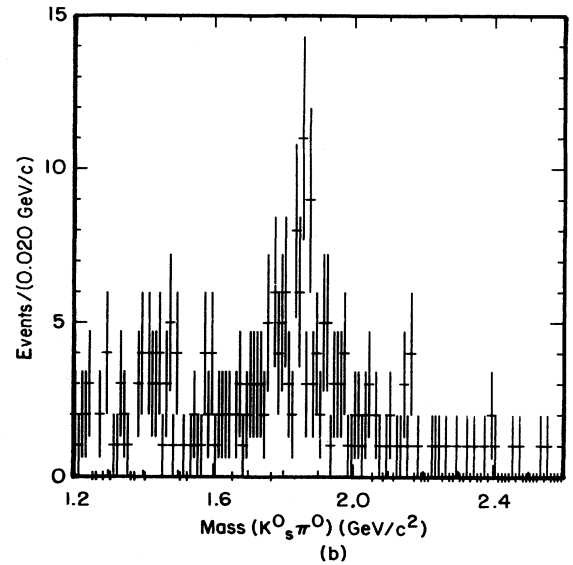
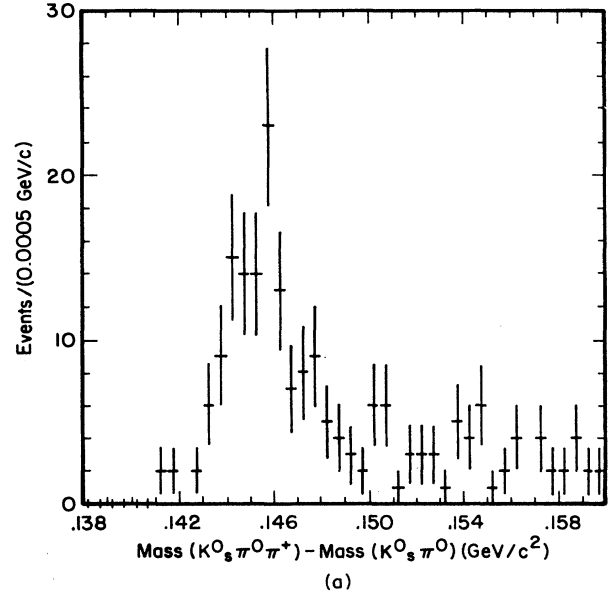


FIG. 3. (a) ΔM for $D^0 \rightarrow K_S^0 \pi^0 \pi^+$ requiring that the $K_S^0 \pi^0$ invariant mass lie in the D^0 region, and (b) the D^0 invariant mass after cutting on ΔM .

mode we are measuring. The number of events for each of these modes is obtained from the ΔM plots and are presented in Table I, along with the relative efficiencies and the resulting ratios of branching ratios. The branching ratios for $D^0 \rightarrow K^- \pi^+ \pi^0$ and $D^0 \rightarrow \bar{K}^0 \pi^0$ obtained from these ratios of branching ratios and Mark III results for $D^0 \rightarrow K^- \pi^+$ and $\bar{D}^0 \rightarrow \bar{K}^0 \pi^+ \pi^-$ are given in Table II.⁸ The agreement between our results and previous experimental results is satisfactory. We have folded into our systematic uncertainty an error ($\approx 25\%$ of our total systematic error) which reflects our uncertainty in interference between the $K^- \rho^+$, $K^{*-} \pi^+$, $\bar{K}^{*0} \pi^0$, and non-resonant $K^- \pi^+ \pi^0$ final states. This is evaluated by run-

TABLE I. Summary of D^0 decays.

D^0 modes	Events	Rel. ϵ	Ratio of branching ratios
$K^- \pi^+ \pi^0 / K^- \pi^+$	$1050 \pm 48 / 2724 \pm 55$	0.14 ± 0.01	$2.8 \pm 0.14 \pm 0.52$
$\bar{K}^0 \pi^0 / \bar{K}^0 \pi^+ \pi^-$	$104.4 \pm 15.4 / 852 \pm 38$	0.34 ± 0.02	$0.36 \pm 0.04 \pm 0.08$
$\bar{K}^{*0} \eta^0 / K^- \pi^+$	$46.5 \pm 15.0 / 2724 \pm 55$	0.034 ± 0.003	$0.58 \pm 0.19^{+0.24}_{-0.28}$
$\bar{K}^0 \omega / \bar{K}^0 \pi^+ \pi^-$	$39.9 \pm 12.2 / 852 \pm 38$	0.087 ± 0.01	$0.54 \pm 0.14 \pm 0.16$
$\bar{K}^0 \pi^+ \pi^- \pi^0 / \bar{K}^0 \pi^+ \pi^-$	$158 \pm 21 / 852 \pm 38$	0.101 ± 0.01	$1.85 \pm 0.26 \pm 0.30$
$K^- \pi^+ \pi^- \pi^+ \pi^0 / K^- \pi^+ \pi^- \pi^+$	$167.4 \pm 19.0 / 4210 \pm 85$	0.072 ± 0.010	$0.55 \pm 0.07^{+0.12}_{-0.09}$

ning a Monte Carlo simulation of these decays according to the parameters measured by the Mark III Collaboration, then observing how our overall result changes with variations in the measured Dalitz-plot parameters.⁹ As Fig. 4 illustrates qualitatively, our data are consistent with the expectation that this final state is dominated by $K^- \rho^+$, consistent with the Mark III results. We have not undertaken a full Dalitz-plot analysis for this decay owing to our large systematic error in this branching ratio, as well as the poorer signal-to-noise ratio as compared with the Mark III analysis.

THE DECAY $D^0 \rightarrow \bar{K}^{*0} \eta$

The decay $D^0 \rightarrow \bar{K}^{*0} \eta$ has been studied previously. To date, there are upper limits on this decay from the ARGUS Collaboration¹⁰ (2.9% at 90%, confidence level) and the E691 Collaboration (1.4% at 90% C.L.).¹¹ We select η through the decay mode $\eta \rightarrow \gamma\gamma$, as outlined above for the π^0 . Our efficiency for reconstruction of the η in the decay mode $\eta \rightarrow \pi^- \pi^+ \pi^0$ is only one-quarter the efficiency in the $\gamma\gamma$ mode, due to the lower momentum of the photons from the π^0 in the former case and greater likelihood of π^+/γ overlap, as well as the relative η branching ratios into these two decay modes. We therefore use only the $\eta \rightarrow \gamma\gamma$ mode to reconstruct candidate η 's. We then combine η candidates with tracks assumed to be K^- and π^+ to form D^0 candidates. For true $D^0 \rightarrow \bar{K}^{*0} \eta$ decays, the \bar{K}^{*0} must be polarized in the helicity-zero state. The ‘‘polarization angle,’’ defined as the angle θ between the direction of one of the \bar{K}^{*0} daughters, measured in the \bar{K}^{*0} rest frame, relative to the direction of the \bar{K}^{*0} , measured in the D^0 frame, must follow a $\cos^2\theta$ distribution. Accordingly, we require that

$|\cos\theta| > 0.4$ in order to improve the signal-to-noise ratio. In Fig. 5, we display the ΔM 's for the $D^0 \rightarrow K^- \pi^+ \eta$ candidates as a function of the $K^- \pi^+$ mass. There is peaking evident in the \bar{K}^{*0} mass interval. To determine how much of the observed peak is due to the two-body decay $\bar{K}^{*0} \eta$, we subtract the ΔM distribution for the \bar{K}^{*0} sideband combinations from the ΔM distribution for the \bar{K}^{*0} candidates, normalized to the region outside of the nominal $D^{*+} - D^{*0}$ mass difference (145.45 MeV), and fit the resulting signal to a Gaussian with the width determined from Monte Carlo calculations (in this case, 3.2 MeV FWHM). The number of events remaining after subtracting this background, and the ratio of

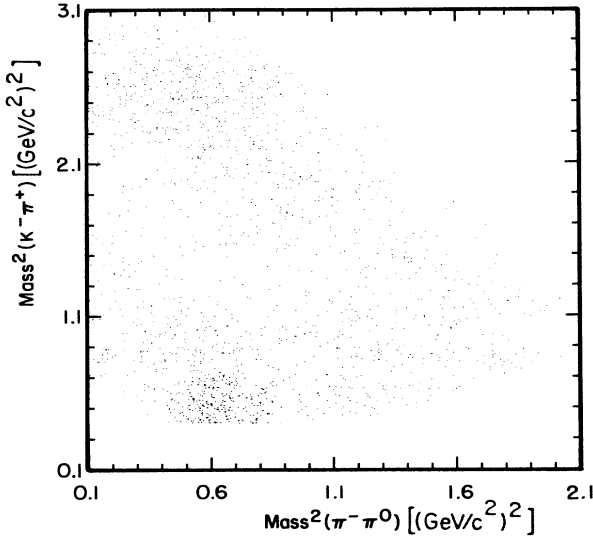
$$B(D^0 \rightarrow \bar{K}^{*0} \eta) : B(D^0 \rightarrow K^- \pi^+)$$

are given in Table I, and the corresponding branching ratio for $D^0 \rightarrow \bar{K}^{*0} \eta$ is given in Table II. As a check, we show in Fig. 6 the same plot for the case where the $\bar{K}^{*0} \eta$ candidate mass falls into the D^0 sideband region. No peaking is observed.

The measurement of $2.3 \pm 0.7^{+1.0}_{-1.1}\%$ of the $D^0 \rightarrow \bar{K}^{*0} \eta$ branching ratio, given in Table II, is consistent with predictions of Bauer *et al.* (3.0%) and of Donoghue¹² ($\geq 2.0\%$) but higher than the quantum chromodynamics (QCD) sum-rule estimate of Blok *et al.* (0.3%).¹³ Interest in this decay mode centers around the possibility that, if the branching ratio for this mode exceeds 2%, it may be at least partially responsible for the large branching ratio observed for the decay mode $D^0 \rightarrow \phi K_S^0$. In such a scheme, the $\bar{K}^{*0} \eta$ state is produced through Fig. 1(a); since the η contains substantial $s\bar{s}$, the η can interact with the \bar{K}^{*0} through quark exchange to produce the vector + pseudoscalar final state ϕK_S^0 .

TABLE II. D^0 decay branching ratios in %.

Mode	Previous B	This expt.	Prediction ²	Prediction ¹³
$K^- \pi^+ \pi^0$	$13.3 \pm 1.2 \pm 1.3^7$	$11.5 \pm 0.6 \pm 2.4$	13.8	15.0
$\bar{K}^0 \pi^0$	$1.9 \pm 0.4 \pm 0.4^7$	$2.3 \pm 0.4 \pm 0.5$	2.4	1.5
$\bar{K}^0 \omega$	$3.7 \pm 1.2^{7,10}$	$3.4 \pm 0.9 \pm 1.0$	2.7	1.5
$\bar{K}^{*0} \eta$	$< 1.4^{11}$	$2.3 \pm 0.7^{+1.0}_{-1.1}$	3.0	
$\bar{K}^0 \pi^+ \pi^- \pi^0$	$11.5 \pm 2.2 \pm 2.8^7$	$10.8 \pm 1.5 \pm 1.7$		
$K^- \pi^+ \pi^- \pi^+ \pi^0$	$5.2 \pm 0.7 \pm 0.6^{11}$	$5.0 \pm 0.7^{+1.3}_{-1.0}$		

FIG. 4. Dalitz distribution for the decay $D^0 \rightarrow K^- \pi^+ \pi^0$.

THE DECAYS $D^0 \rightarrow K^- \pi^+ \pi^- \pi^+ \pi^0$ AND $D^0 \rightarrow \bar{K}^0 \omega$

We search for the D^0 in the final states $K^- \pi^+ \pi^- \pi^+ \pi^0$ and $K_S^0 \pi^+ \pi^- \pi^0$ and, in the latter case, consider substructure in the $\pi^+ \pi^- \pi^0$ system. The decay $\bar{K}^0 \omega$ has already been observed by both the Mark III and ARGUS Collaborations with a sizable branching ratio $[(3.2 \pm 1.3 \pm 0.8)\%$ and $(4.2 \pm 1.6 \pm 0.9)\%$, respectively].¹⁰ In the context of a QCD sum-rule calculation, this branching ratio is expected to be on the order of 0.4%,¹³ other theoretical predictions for this mode vary between 2.7 (Ref. 2) and 3.0%.¹²

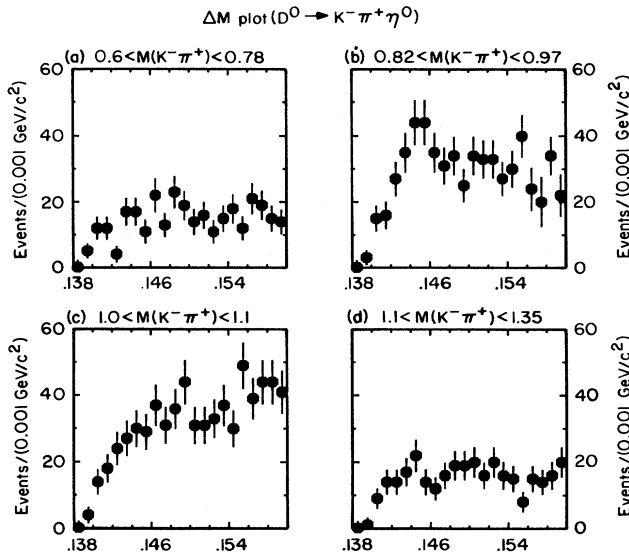
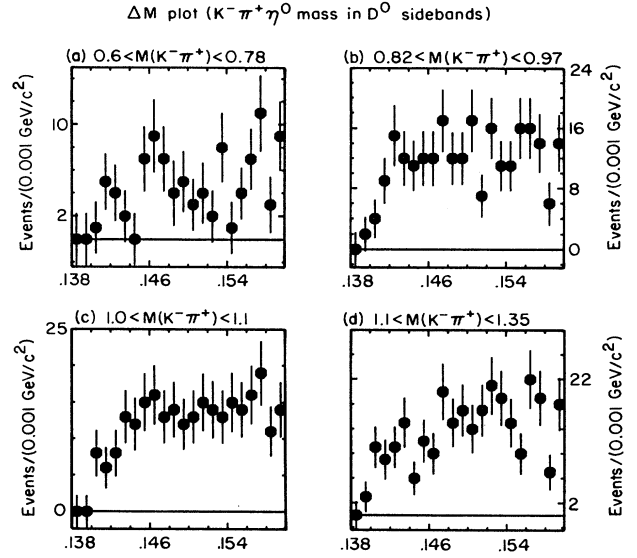
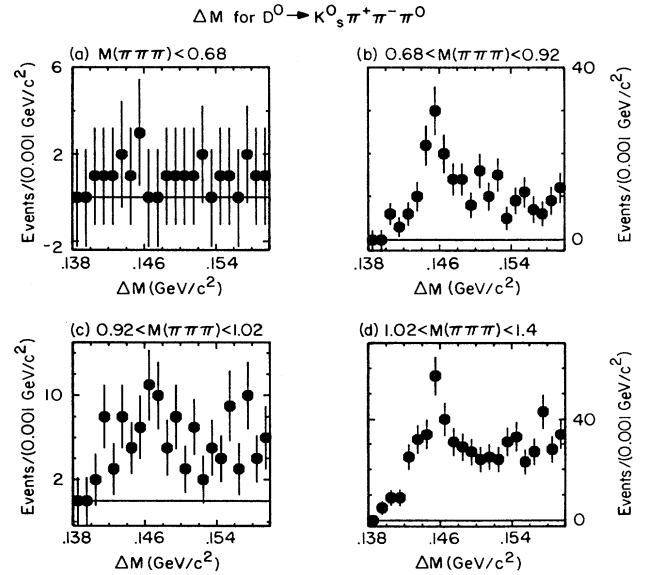
FIG. 5. ΔM for $D^0 \rightarrow K^- \pi^+ \eta$ candidates for $K^- \pi^+$ invariant mass (a) below, (b) consistent with, and (c) and (d) above the $\bar{K}^0 \omega$ mass region.FIG. 6. ΔM corresponding to previous plot for candidates where D^0 invariant mass lies in D^0 sideband regions.

Figure 7 displays the ΔM for the $D^0 \rightarrow K_S^0 \pi^- \pi^+ \pi^0$ candidates, again plotted in separate $M(\pi^+ \pi^- \pi^0)$ intervals. Integrating over all $\pi^+ \pi^- \pi^0$ masses, we obtain a total branching ratio of $(10.8 \pm 1.5 \pm 1.7)\%$ for the final state $\bar{K}^0 \pi^+ \pi^- \pi^0$, consistent with the Mark III measurement⁷ for this decay $[(11.5 \pm 2.2 \pm 2.8)\%]$. We notice a clear signal in the $\pi^+ \pi^- \pi^0$ mass region consistent with the ω mass. By subtracting the ω sideband contribution (amounting to $10 \pm 10\%$ of our observed signal), we obtain a branching ratio of $(3.4 \pm 0.9 \pm 1.0)\%$ for the

FIG. 7. Signal for $D^0 \rightarrow K_S^0 \pi^- \pi^+ \pi^0$ candidates in which $M(\pi^+ \pi^- \pi^0)$ is (a) less than, (b) consistent with, and (c) and (d) greater than the ω mass.

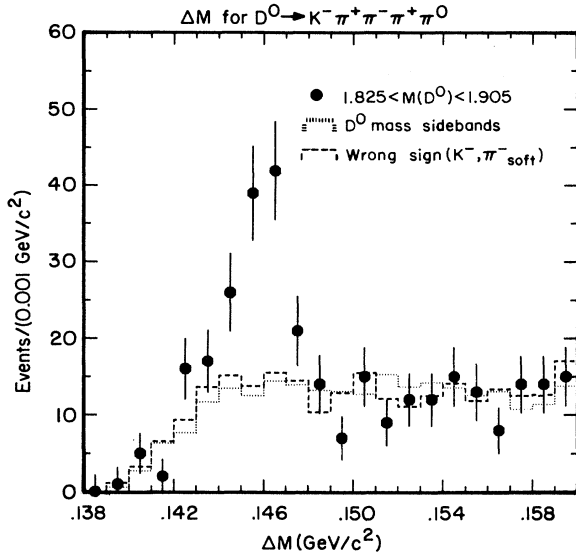


FIG. 8. ΔM for $D^0 \rightarrow K^- \pi^+ \pi^- \pi^+ \pi^0$ candidates with various estimators of the back-ground overplotted.

$D^0 \rightarrow \bar{K}^0 \omega$ decay mode, in good agreement with the ARGUS and Mark III measurements. There is also a peaking evident at large values of $M(\pi^- \pi^+ \pi^0)$. Monte Carlo studies indicate that this peaking is consistent with $K_S^0 a_1$ as well as $K_S^0 \pi^- \pi^+ \pi^0$, where the three pions have a phase-space invariant-mass distribution.

Decays of D mesons into a kaon plus four pions have already been observed for both the D^+ and D^0 ,^{14,15} albeit with poor statistics. The E691 Collaboration¹¹ has recently remeasured this branching ratio to be $(5.2 \pm 0.7 \pm 0.6)\%$. Figure 8 displays the candidate $K^- \pi^+ \pi^- \pi^+ \pi^0$ signal. Because of the larger combinatoric background in this case, we have made a cut of $x_D > 0.6$ rather than the usual $x_D > 0.5$. We fit this distribution to the sum of a Gaussian signal plus a background obtained from the ΔM plot we obtain for events where the kaon (which tags the flavor of the D^0/\bar{D}^0) and the slow pion from $D^{*+} \rightarrow D^0 \pi^+$ have the wrong-sign correlation. We thereby determine the signal size to be 167 ± 19 events. We have examined the possibility that there is contamination from other sources, such as the copious $D^0 \rightarrow K^- \pi^+ \pi^- \pi^+$ decay chains, by running a Monte Carlo simulation of continuum $c\bar{c}$ events, where we exclude the $D^0 \rightarrow K^- \pi^+ \pi^- \pi^+ \pi^0$ final state, and con-

sider a possible signal arising from real D^0 daughters paired with random π^0 's in the same event. Such a Monte Carlo study indicates that this effect accounts for less than 5% of our observed signal. Normalizing to the signal we observe in $D^0 \rightarrow K^- \pi^+ \pi^- \pi^+$, we derive an overall branching ratio of $(5.0 \pm 0.7_{-1.0}^{+1.3})\%$ for the decay $D^0 \rightarrow K^- \pi^+ \pi^- \pi^+ \pi^0$ (Table II), consistent with previous measurements.

CONCLUSIONS

We have investigated D^0 decays to several final states, comparing with theoretical predictions for two-body decay modes. The decay mode $\bar{K}^0 \pi^0$ is observed with a branching ratio in excess of expectations based on simple color-matching requirements. It is interesting to note that, if the exchange diagram and the spectator diagrams were, in fact, of equal strength, we would expect a branching ratio for $\bar{K}^0 \pi^0$ of 2%, in agreement with our observation. The QCD sum-rule prediction of 1% is lower than our finding. We find $\bar{K}^0 \omega$ at a level roughly $1.5 \times \bar{K}^0 \pi^0$, generally consistent with the trend observed in D^0 decays where VP final states are favored over PP final states. The decay mode $\bar{K}^{*0} \eta$ is observed with a branching ratio comparable to $\bar{K}^0 \pi^0$ which is consistent with models suggesting that this mode is feeding into ϕK_S^0 . Owing to the fact that the η contains both $s\bar{s}$ as well as $u\bar{u}$ and $d\bar{d}$ components in its quark wave function, this mode is accessible to diagrams which lead to both the $\bar{K}^0 \pi^0$ as well as the $\bar{K}^0 \phi$ final state. The mode $K^- \pi^+ \pi^- \pi^+ \pi^0$ is observed with a branching ratio of $\approx 5\%$, roughly $\frac{1}{5}$ of the as yet unaccounted for exclusive D^0 final states. We find, in general, that the BSW model seems to fit very well to all our observations, supporting the viability of the hypothesis that destructive interference between two D^+ decay diagrams is responsible for the longer lifetime of the D^+ relative to the D^0 .

ACKNOWLEDGMENTS

We gratefully acknowledge the effort of the Cornell Electron Storage Ring staff. P.S.D. thanks the Presidential Young Investigation program of the National Science Foundation (NSF), and R.P. thanks the A. P. Sloan Foundation for support. This work was supported by the National Science Foundation and the U.S. Department of Energy under Contract Nos. DE-AC0276ER0(1428, 3064, 1545), DE-AC02(78ER05001, 83ER40105), and DE-FG0586ER40272. The supercomputing resources of the Cornell Theory Center were used in this research.

¹Particle Data Group, J. J. Hernández *et al.*, Phys. Lett. B **239**, 1 (1990).

²M. Bauer *et al.*, Z. Phys. C **34**, 103 (1987).

³J. P. Cúmalat *et al.*, Phys. Lett B **210**, 253 (1988); CLNS Report No. 89-940 (unpublished).

⁴H. Albrecht *et al.*, Phys. Lett. **158B**, 525 (1986); R. M. Baltusaitas *et al.*, Phys. Rev. Lett. **56**, 2136 (1986); C. Bebek *et al.*, *ibid.* **56**, 1893 (1986).

⁵D. G. Cassel *et al.*, Nucl. Instrum. Methods A **252**, 325 (1986).

⁶CLEO Collaboration, S. Behrends *et al.*, Phys. Rev. D **31**, 2161 (1985).

⁷J. Adler *et al.*, Phys. Rev. Lett. **60**, 89 (1988); D. Hitlin, in *Lepton and Photon Interactions*, proceedings of the International Symposium on Lepton and Photon Interactions at High Energies, Hamburg, West Germany, 1987, edited by W. Bartel and R. Rückl [Nucl. Phys. B (Proc. Suppl.) **3** (1987)].

⁸The systematic errors shown on the branching ratios obtained in Table II do not include the errors on the modes to which

our branching ratios are being normalized.

⁹J. Adler *et al.*, Phys. Lett. B **196**, 107 (1987).

¹⁰H. Albrecht *et al.*, Z. Phys. C **43**, 181 (1989).

¹¹J. C. Anjos *et al.* Phys. Rev. D **42**, 2414 (1990).

¹²J. F. Donoghue, Phys. Rev. D **33**, 1516 (1986).

¹³B. Yu. Blok and M. A. Shifman, Yad. Fiz. **45**, 841 (1987) [Sov. J. Nucl. Phys. **45**, 522 (1987)].

¹⁴M. Aguilar-Benitez *et al.*, Z. Phys. C **31**, 491 (1986).

¹⁵S. Barlag *et al.*, Phys. Lett. B **232**, 561 (1989).